

ULRR

Evaluation of potassium glycinate, potassium lysinate, potassium sarcosinate and potassium threonate solutions in CO₂ capture using membranes

Item Type	Article
Authors	Marjani, Azam;Nakhjiri, Ali Taghvaie;Pishnamazi, Mahboubeh;Shirazian, Saeed
Citation	Arabian Journal of Chemistry;14, 102979
Publisher	Elsevier
Download date	2026-05-09 13:27:13
Item License	https://creativecommons.org/licenses/by-nc-sa/1.0/
Link to Item	https://hdl.handle.net/10344/9669



ORIGINAL ARTICLE

Evaluation of potassium glycinate, potassium lysinate, potassium sarcosinate and potassium threonate solutions in CO₂ capture using membranes



Azam Marjani^{a,b}, Ali Taghvaie Nakhjiri^c, Mahboubeh Pishnamazi^{d,e,f,*},
Saeed Shirazian^{f,g}

^a Department for Management of Science and Technology Development, Ton Duc Thang University, Ho Chi Minh City, Viet Nam

^b Faculty of Applied Sciences, Ton Duc Thang University, Ho Chi Minh City, Viet Nam

^c Department of Petroleum and Chemical Engineering, Science and Research Branch, Islamic Azad University, Tehran, Iran

^d Institute of Research and Development, Duy Tan University, Da Nang 550000, Viet Nam

^e The Faculty of Pharmacy, Duy Tan University, Da Nang 550000, Viet Nam

^f Department of Chemical Sciences, Bernal Institute, University of Limerick, Limerick, Ireland

^g Laboratory of Computational Modeling of Drugs, South Ural State University, 76 Lenin prospekt, 454080 Chelyabinsk, Russia

Received 17 October 2020; accepted 27 December 2020

Available online 06 January 2021

KEYWORDS

Mass transfer;
Numerical simulation;
Separation;
Process modeling

Abstract The mitigation process of greenhouse gases emission such as CO₂ into the atmosphere is known as a vital necessity in modern societies. Nowadays, amino acid salt solutions (AASSs) have been extensively applied as a promising alternative to alkanol amine absorbents to increase the CO₂ sequestration efficiency from disparate gaseous flows. This article aims to computationally and theoretically evaluate the CO₂ separation percentage using potassium glycinate (PG), potassium lysinate (PL), potassium sarcosinate (PS) and potassium threonate (PT) amino acid solutions from an inlet gaseous mixture inside a hydrophobic membrane contactor (HMC). To do this, the governing first principal equations inside the HMC are solved using the computational fluid dynamics procedure based on finite element technique. Acceptable agreement between the simulation results and experimental values with average deviation of approximately 3% implies the validation of developed two-dimensional (2D) simulation approach developed in this study. The analysis of obtained results demonstrated that PG is the most efficient amino acid solution for CO₂ molecular sequestration with the ability of separating 90% of inlet CO₂ in the system. The order of solutions is

* Corresponding author at: Duy Tan University, Da Nang 550000, Viet Nam.

E-mail address: mahboubehpishnamazi@duytan.edu.vn (M. Pishnamazi).

Peer review under responsibility of King Saud University.



90% sequestration using PG > 89.3% sequestration using PT > 77.4% sequestration using PL > 72.3% sequestration using PS.

© 2021 The Author(s). Published by Elsevier B.V. on behalf of King Saud University. This is an open access article under the CC BY license (<http://creativecommons.org/licenses/by/4.0/>).

1. Introduction

Over the previous decades, boundless increment in humans' industrial activities has eventuated in significant challenges associated with the emission of poisonous greenhouse gases (mainly CO₂) into the atmosphere such as air contamination and climate change (Herzog et al., 2000; Nakhjiri and Heydarinasab, 2019; Rongwong et al., 2013).

CO₂ is known as the most prominent component of greenhouse contaminants based on the Intergovernmental Panel on Climate Change (IPCC) (Mehdipour et al., 2014). Therefore, numerous conventional techniques such as cryogenic separation and absorption towers have been proposed to appropriately separate CO₂ and control its perilous influences on the humans' health (Nakhjiri et al., 2018a; Park et al., 2009; Rufford et al., 2012). Despite having acceptable performance of CO₂ sequestration and commercial viability, conventional technologies have lost their applicability to purify gas streams containing carbon dioxide, due to possessing unfavorable drawbacks such as foaming, channeling, and high operational costs (Demontigny et al., 2005; Kreulen et al., 1993; Pishnamazi et al., 2020a). The emergence of hydrophobic membrane contactors (HMCs) as a novel gas-liquid contact technology has been significantly promising for investigators to enhance the CO₂ sequestration percentage due to their novel privileges such as modularity and great flexibility in managing gas-liquid flow rates (Ghadiri et al., 2018; Nakhjiri et al., 2018c, 2020; Shirazian et al., 2012).

Recently, development of numerical modeling and computational simulations associated with HMCs based on the computational fluid dynamics (CFD) approach has been of great interest due to enabling researchers to perceive the unpredicted parameters such as wettability and membrane porosity which influence the final efficiency of HMCs. For instance, Nasim Afza et al. developed a dynamic model to investigate CO₂ removal efficiency applying liquid water as absorbent inside a porous membrane contactor. They found that enhancing the velocity of liquid from 0.1 to 0.45 m s⁻¹ increased the mass transfer flux from 8×10^{-4} to almost 17×10^{-4} mol m⁻² s⁻¹, which was in great agreement with the employed measured data (Afza et al., 2018). Zhang et al. developed a numerical simulation to assess the removal yield of CO₂ inside a HMC. They applied the mixture of methyldiethanolamine (MDEA) and 2-(1-piperaziny)-ethylamine (PZEA) to chemically sequester CO₂. They found that by increasing the number of fibers from 3000 to 10,000 substantially enhance the CO₂ separation yield from 47.8 to 98.1% (Zhang et al., 2014).

Liquid chemical absorbents play a noteworthy role in CO₂ sequestration process. For decades, alkanolamine chemical solutions such as monoethanolamine (MEA), methyldiethanolamine (MDEA), ethylenediamine (EDA) and ethylethanolamine (EEA) have been widely utilized for sequestering CO₂ through the HMCs. But, the existence of major operational negative points such as corrosiveness, thermal degradation

and the need of high amount of energy for regeneration have persuaded the researchers to look for novel liquid absorbents to overcome the aforementioned disadvantages (Blauwhoff et al., 1983; Faiz and Al-Marzouqi, 2009; Kim and Yang, 2000; Razavi et al., 2013). Amino acid salt solutions (AASSs) have been recently selected as an interesting alternative for alkanolamine absorbents due to their outstanding capabilities such as superior stability in the exposure to oxygen, lower volatility and acceptable regeneration ability (Afza et al., 2018; Kumar et al., 2003; Nakhjiri and Heydarinasab, 2020a). Razavi et al. proposed a computational simulation of a HMC to measure the sequestration percentage of CO₂ from N₂/CO₂ gaseous mixture applying potassium threonate (PT) absorbent. They reported that increase in the absorbent flow rate from 50 to 350 cm³ min⁻¹ improved the CO₂ flux from 2×10^{-4} to 2.4×10^{-4} kmol m⁻² s⁻¹ (Razavi et al., 2016). Van Holst et al. performed an experimental investigation for studying the CO₂ absorption kinetics in eight disparate amino acid salt solutions. They concluded that the potassium sarcosinate and potassium proline possessed great reaction rate towards CO₂ removal (van Holst et al., 2009).

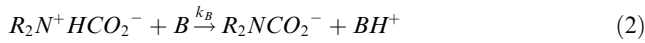
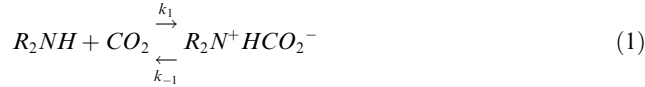
In economic viewpoint, HMCs have been currently known as an appropriate alternative for traditional CO₂ absorption technologies such as cryogenic separation and absorption towers due to their significant potential to employ the advantages of both chemical absorption and membrane separation technology with great performance (Feron et al., 1992; Naim et al., 2012; Nakhjiri et al., 2020). Zhou et al. provided an economical comparison between the traditional gas-liquid contactors (i.e. spray towers) with novel membrane contactors such as HMCs. They corroborated the HMCs possess the great potential to save the operating cost by about 40%, which is able to be justified due to their superior specific surface area and better flexibility to control gas-liquid flow rates compared to the conventional gas-liquid contacting systems (Li et al., 2013; Zhou et al., 2010).

The important aim of this paper is to numerically develop a modeling and computationally assemble a two-dimensional (2D) axisymmetrical simulation based on the computational fluid dynamics (CFD) procedure to investigate the amount of CO₂ molecular sequestration applying various AASSs inside the HMC. As the novelty, four novel AASSs including potassium sarcosinate (PS), potassium glycinate (PG), potassium lysinate (PL) and PT are applied and consequently compared to introduce the best solution for CO₂ separation. Membrane porosity/tortuosity, length of module and gas flow rate are considered as important operational parameters, which are aimed to be studied to evaluate their effects on the CO₂ sequestration yield.

2. Chemical reaction of CO₂ with different AASSs

It is important to note that the reaction rate equation of CO₂ molecules with the employed AASSs (PT, PG, PS and PL)

seems to be necessary for developing the wide-ranging simulation. Generally, it can be claimed that the pathway of CO₂ molecules-AASSs reaction is similar to the CO₂ molecules-amine reaction due to the similarity of AASSs molecular structure with primary amines (Kumar et al., 2003). The zwitterionic and termolecular reaction mechanisms are known as the most authentic mechanisms for interpreting the CO₂ molecules-AASSs reaction (Caplow, 1968; Crooks and Donnellan, 1989). Based on the zwitterionic mechanism, CO₂ binding with AASSs forms a zwitterion. Then, the instant deprotonation process of zwitterion takes place by H⁺ ion exchange with water or a base associated with the solution. The following reactions present the zwitterions formation/deprotonation, respectively (Caplow, 1968; Danckwerts, 1979):



where B stands for the base, capable to deprotonate the zwitterions. In AASSs, H₂O and OH⁻ are the desired bases. The chemical reaction rates of CO₂ molecules with PT, PG, PS and PL amino acid salt solutions inside the tube pathway of HMC are presented as follows (Aronu et al., 2011; Portugal et al., 2007b, 2008; Shen et al., 2016):

$$r_{CO_2-PT} = -4.13 \times 10^8 \exp(-3580/T) C_{PT} \exp(0.9 C_{PT}) C_{CO_2} \quad (3)$$

$$r_{CO_2-PG} = -(2.42 \times 10^{16} \exp(-8544/T) \exp(0.44 C_{PG}) C_{PG} C_{CO_2}) \quad (4)$$

$$r_{CO_2-PS} = -\frac{C_{PS} C_{CO_2}}{(1/k') + (1/(k_{PS} C_{PS} + k_{H_2O} C_{H_2O}))} \quad (5)$$

$$r_{CO_2-PL} = -(2.778 \times 10^{13} \exp(-6138/T)) C_{PL} C_{CO_2} \quad (6)$$

3. Modeling and simulation

In the present investigation, a mechanistic/mathematical modeling and an axisymmetrical 2D simulation are developed to theoretically evaluate the dynamic CO₂ molecular sequestration from an inlet gaseous mixture using PT, PG, PS and PL amino acid salt solutions inside the HMC. Each commercial module consists of a microporous hydrophobic membrane that causes separation of the gas-liquid phases. The occurrence of CO₂ molecular mass transfer may be justified by the diffusion of CO₂ molecules existed in the feed gas (inside the shell compartment) to the membrane walls and consequently their chemical absorption via AASSs inside the tube pathway. Fig. 1 schematically depicts the CO₂ molecular mass transfer, simplified geometry and module cross section of a HMC.

The followings are considered as the functional assumptions employed for simplifying the development of model and wide-ranging simulation (Al-Marzouqi et al., 2008a; Ghadiri et al., 2018; Zhang, 2016; Zhang et al., 2014):

- 1) Steady state and isothermal modes of operation;
- 2) The deprotonation process is assumed to be fast;
- 3) The CO₂ molecules manner is considered First-order;
- 4) Microporous membrane is assumed to be non-selective;
- 5) The identical distribution of membrane pores inside the HMC;

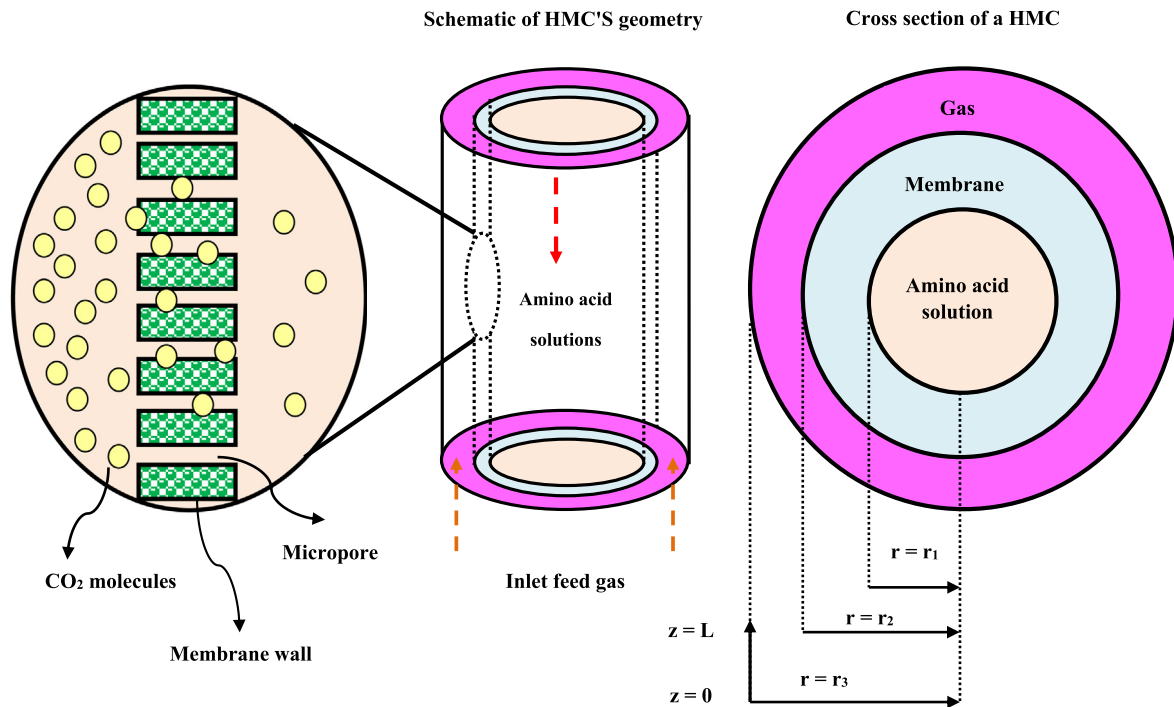


Fig. 1 The CO₂ molecular mass transfer, simplified geometry and module cross section of a HMC.

- 6) The membrane module is assumed Axisymmetrical in the simulations;
- 7) Membrane pores are only filled with gas (Non-wetted mode of operation);
- 8) Henry's law is employed to interpret the gas phase - amino acid solutions' equilibrium;
- 9) The gas phase in the shell pathway is assumed to follow the ideal demeanor;
- 10) It is assumed that the AASSs inside the tube compartment and inlet feed gas in the shell pathway follow the laminar flow regime;
- 11) AASSs and gaseous mixture flow counter-currently.

Table 1 represents the essential HMC's specifications and employed operating conditions. COMSOL software is well identified as an appropriate commercial package to simultaneously solve the main partial differential equations (PDEs) in prominent segments of HMC using finite element technique (FET). Based on this aim, PARDISO numerical solver has been well determined as a suitable solver to analyze the governing PDEs due to some advantages such as simplicity, robustness and capability to solve stiff/non-stiff boundary problems. In order to solve the PDEs, a platform with a 64-bit operating system, an Intel core™ i5-4200U CPU at 2.67 GHz and a 4 Gigabyte RAM is applied. It is worth noting that the running duration (computational time) of this geometry using the aforementioned solver was about 8 min.

The basic mass transfer equation based on non-wetted and steady state operational modes for components i including CO₂ molecules and disparate AASSs (PG, PL, PS and PT) inside the tube of HMC is derived as follows (Faiz and Al-Marzouqi, 2009; Nakhjiri et al., 2018b; Pishnamazi et al., 2020c; Pishnamazi et al., 2020d):

$$D_{i,tube} \left[\frac{\partial^2 C_{i,tube}}{\partial r^2} + \frac{1}{r} \frac{\partial C_{i,tube}}{\partial r} + \frac{\partial^2 C_{i,tube}}{\partial z^2} \right] + R_i = V_{z,tube} \frac{\partial C_{i,tube}}{\partial z} \quad (7)$$

where, the diffusion coefficients of CO₂ molecules and all of the employed AASSs including PT, PG, PS and PL in the HMC's tube section is defined with $D_{i,tube}$. Also, the reaction rate and axial velocity are interpreted with R_i and $V_{z,tube}$, respectively. Newtonian laminar flow regime is assumed inside the tube.

Table 1 The essential HMC's specifications and employed operating conditions (Yan et al., 2007).

Parameter	Unit	Value
Inner hollow fiber radius (r_1)	m	1.72×10^{-4}
Outer hollow fiber radius (r_2)	m	2.21×10^{-4}
Module inner radius	m	0.04
Porosity (ϵ)	-	0.45
Module length (L)	m	1
Number of fibers (n)	-	7000
AASSs temperature (T)	K	308
AASSs concentration (C_{AASSs})	mol m ⁻³	1000
Gas flow rate (V_g)	m s ⁻¹	0.211
Liquid flow rate (V_l)	m s ⁻¹	0.0503
CO ₂ volume fraction in feed gas	vol.%	14
Packing density ($1-\phi$)	%	21.4
Average pore size	µm	0.02×0.2

Therefore, the following equation defines the axial velocity distribution (Faiz and Al-Marzouqi, 2009; Nakhjiri et al., 2018a):

$$V_{z,tube} = 2 \bar{V}_l \left[1 - \left(\frac{r}{r_1} \right)^2 \right] \quad (8)$$

where the amount of average velocity in the tube, radial coordinate and the radius of inner fibers are expressed by \bar{V}_l , r and r_1 , respectively. Employed boundary conditions in the tube pathway can be interpreted as follows:

$$at \ r = 0 : \partial C_{CO_2,tube} / \partial r = 0 \quad (9)$$

$$at \ r = r_1 : C_{CO_2,tube} = m_{CO_2} C_{CO_2,mem} \quad (10)$$

$$at \ z = 0 : \text{Convective flux} \quad (11)$$

$$at \ z = L : C_{CO_2,tube} = 0, C_{solution,tube} = C_{initial} \quad (12)$$

The fundamental mass transfer equation based on non-wetted and steady state operational modes inside the membrane pathway of HMC is presented by Eq. (13) (Faiz and Al-Marzouqi, 2009; Nakhjiri et al., 2018a; Pishnamazi et al., 2020b). In this investigation, polypropylene membrane is applied due to its brilliant hydrophobic property. The appropriate hydrophobicity of porous membrane results in facilitating the penetration of CO₂ molecules into the wall pores of membrane. By the assumption of non-wetted operational mode, membrane pores are only filled with the gas molecules. Therefore, the diffusion of CO₂ molecules inside the gas is the only mass transfer mechanism through the membrane micropores (Afza et al., 2018; Al-Marzouqi et al., 2008b; Nakhjiri and Roudsari, 2016; Pishnamazi et al., 2020d; Shirazian et al., 2020).

$$D_{CO_2,mem} \left[\frac{\partial^2 C_{CO_2,mem}}{\partial r^2} + \frac{1}{r} \frac{\partial C_{CO_2,mem}}{\partial r} + \frac{\partial^2 C_{CO_2,mem}}{\partial z^2} \right] = 0 \quad (13)$$

where the amount of CO₂ concentration and molecular diffusion coefficient in the membrane micropores are denoted with $C_{CO_2,mem}$ and $D_{CO_2,mem}$, respectively. As may be well perceived, $D_{CO_2,mem}$ is an important parameter, which respectively possesses direct connection with membrane porosity (ϵ) and reverse connection with membrane tortuosity (τ) and can be derived as (Faiz and Al-Marzouqi, 2009; Nakhjiri et al., 2018a):

$$D_{CO_2,mem} = \frac{\epsilon D_{CO_2,shell}}{\tau} \quad (14)$$

$D_{CO_2,shell}$ in the aforementioned equation stands for the CO₂ molecular diffusion coefficient in the shell of HMC. Utilized boundary conditions in the membrane pathway is interpreted as follows:

$$at \ r = r_1 : C_{CO_2,mem} = C_{CO_2,tube} / m_{CO_2} \quad (15)$$

$$at \ r = r_2 : C_{CO_2,mem} = C_{CO_2,shell} \quad (16)$$

$$at \ z = 0 : \text{Insulated} \quad (17)$$

$$at \ z = L : \text{Insulated} \quad (18)$$

To derive the basic mass transfer equation based on non-wetted and steady state operational modes inside the shell pathway of HMC for the CO₂ molecular transport, either Maxwell-Stefan theory or Fick's law is able to be applied as follows (Al-Marzouqi et al., 2008a; Eslami et al., 2011):

$$D_{CO_2,s} \left[\frac{\partial^2 C_{CO_2,s}}{\partial r^2} + \frac{1}{r} \frac{\partial C_{CO_2,s}}{\partial r} + \frac{\partial^2 C_{CO_2,s}}{\partial z^2} \right] = V_{z,s} \frac{\partial C_{CO_2,s}}{\partial z} \quad (19)$$

Assumption of gas phase's laminar flow regime and Happel's free surface model in the porous HMC eventuated in the derivation of the velocity profile via the following equation (Eslami et al., 2011):

$$V_{z,shell} = 2 \bar{V}_s \left[1 - \left(\frac{r_2}{r_3} \right)^2 \right] \times \left[\frac{(r/r_3)^2 - (r_2/r_3)^2 + 2 \ln(r_2/r)}{3 + (r_2/r_3)^4 - 4(r_2/r_3)^2 + 4 \ln(r_2/r_3)} \right] \quad (20)$$

In the above equation, the velocity in the z (axial) direction, the shell pathway's average velocity and the radius of outer fiber in HMC are respectively signified by $V_{z,shell}$ and \bar{V}_s and r_2 . Furthermore, the shell pathway's hypothetical effective radius is denoted by r_3 and predicted as follows (Faiz and Al-Marzouqi, 2009; Nakhjiri and Heydarinasab, 2020a):

$$r_3 = r_2 \sqrt{1/(1-\varphi)} \quad (21)$$

In the aforementioned equation, $(1-\varphi)$ stands for the packing density in the HMC and is calculated as (Nakhjiri and Heydarinasab, 2019; Razavi et al., 2016):

$$1 - \varphi = \frac{nr_2^2}{R^2} \quad (22)$$

In Eq. (22), the module inner radius and the fibers number embedded in the module are respectively defined with R and n . Additionally, r_3 is calculated as 4.78×10^{-4} m applying the mixture of Eqs. (21) and (22). Employed boundary conditions in the shell pathway are rendered as follows:

$$\text{at } r = r_2 : C_{CO_2,shell} = C_{CO_2,mem} \quad (23)$$

$$\text{at } r = r_3 : \partial C_{CO_2,shell} / \partial r = 0 \quad (24)$$

$$\text{at } z = 0 : C_{CO_2,shell} = C_{initial} \quad (25)$$

$$\text{at } z = L : \text{Convective flux} \quad (26)$$

The essential physicochemical parameters related to CO_2 gas and PT, PG, PS and PL amino acid salt solutions are listed in Table 2.

4. Study of flow regime inside the HMC

In this paper, the dimensionless Reynolds (Re) number of AASSs and gaseous mixture is scheduled to be calculated in both tube and shell compartments of HMC to study the laminar flow pattern. The following equation represents the Re

Table 2 The essential physicochemical parameters related to CO_2 gas and PT, PG, PS and PL amino acid salt solutions.

Parameter	Value	Unit	Reference
$D_{CO_2,shell}$	1.8×10^{-5}	$m^2 s^{-1}$	(Faiz and Al-Marzouqi, 2009)
$D_{CO_2,mem}$	$D_{CO_2,shell}(\varepsilon/\tau)$	$m^2 s^{-1}$	(Faiz and Al-Marzouqi, 2009)
$D_{CO_2,PT}$	1.38×10^{-9}	$m^2 s^{-1}$	(Shen et al., 2013)
$D_{CO_2,PG}$	1.8×10^{-9}	$m^2 s^{-1}$	(Portugal et al., 2007a)
$D_{CO_2,PS}$	1.547×10^{-9}	$m^2 s^{-1}$	(Aronu et al., 2011)
$D_{CO_2,PL}$	9×10^{-10}	$m^2 s^{-1}$	Calculated from (Shen et al., 2016)
$D_{PT,tube}$	8.45×10^{-10}	$m^2 s^{-1}$	(Constantinou et al., 2014)
$D_{PG,tube}$	$0.5 \times D_{CO_2,PG}$	$m^2 s^{-1}$	Estimated (Faiz and Al-Marzouqi, 2009; Ghasem and Al-Marzouqi, 2017)
$D_{PS,tube}$	1.03×10^{-9}	$m^2 s^{-1}$	(Hamborg et al., 2008)
$D_{PL,tube}$	$0.5 \times D_{CO_2,PG}$	$m^2 s^{-1}$	Estimated (Faiz and Al-Marzouqi, 2009; Ghasem and Al-Marzouqi, 2017)
$m_{CO_2,PT}$	1.5	–	(Portugal et al., 2008)
$m_{CO_2,PG}$	0.625	–	Calculated from (Portugal et al., 2009)
$m_{CO_2,PS}$	0.544	–	Calculated from (Aronu et al., 2011; Eslami et al., 2011)
$m_{CO_2,PL}$	0.602	–	Calculated from (Eslami et al., 2011; Shen et al., 2016)
k'	$2.6198 \times 10^9 \exp(-915.8/T)$	$m^3 kmol^{-1} s^{-1}$	(Aronu et al., 2011)
k_{PS}	$6.3494 \times 10^6 \exp(-1589.6/T)$	$m^6 kmol^{-2} s^{-1}$	(Aronu et al., 2011)
k_{H_2O}	$3.9805 \times 10^8 \exp(-3924.4/T)$	$m^6 kmol^{-2} s^{-1}$	(Aronu et al., 2011)
μ_{PG}	0.964×10^{-3}	$Pa s^{-1}$	(Lu et al., 2011)
μ_{PL}	1.445×10^{-3}	$Pa s^{-1}$	Calculated from (Mazinani et al., 2015)
μ_{PT}	1.148×10^{-3}	$Pa s^{-1}$	Calculated from (Portugal et al., 2008)
μ_{PS}	0.35×10^{-3}	$Pa s^{-1}$	Calculated from (Majchrowicz, 2014)
μ_{CO_2}	1.52×10^{-5}	$Pa s^{-1}$	(Bar-Meir, 2014)
μ_{CH_4}	1.13×10^{-5}	$Pa s^{-1}$	(Bar-Meir, 2014)
$\mu_{gaseousmixture}$	$(0.14 \times \mu_{CO_2} + 0.86 \times \mu_{CH_4})$	$Pa s^{-1}$	(Bar-Meir, 2014)
ρ_{PG}	1061.9	$kg m^{-3}$	(Lu et al., 2011)
ρ_{PL}	1072	$kg m^{-3}$	(Mazinani et al., 2015)
ρ_{PT}	1062.5	$kg m^{-3}$	(Portugal et al., 2008)
ρ_{PS}	1260	$kg m^{-3}$	Calculated from (Majchrowicz, 2014)
ρ_{CO_2}	1.75	$kg m^{-3}$	(Bar-Meir, 2014)
ρ_{CH_4}	0.64	$kg m^{-3}$	(Bar-Meir, 2014)
$\rho_{gaseousmixture}$	$(0.14 \times \rho_{CO_2} + 0.86 \times \rho_{CH_4})$	$kg m^{-3}$	(Bar-Meir, 2014)

number for PG, PL, PS and PT AASSs inside the tube of HMC (Bird et al., 1960; Nakhjiri et al., 2020):

$$Re_l = \frac{\rho_l V_l D_i}{\mu_l} \quad (27)$$

In the abovementioned equation, ρ_l , μ_l and V_l are, respectively, expressed as density, viscosity, and velocity of AASSs, respectively. Moreover, D_i is the fiber's inner diameter. The Re number for CO₂/CH₄ gaseous mixture flowing inside the shell of HMC is predicted using the following equation (Bird et al., 1960; Nakhjiri et al., 2020):

$$Re_g = \frac{\rho_g V_g D_h}{\mu_g} \quad (28)$$

where ρ_g , V_g , μ_g and D_h are respectively denoted as gaseous mixture's density, velocity, viscosity, and shell's hydraulic diameter. Table 3 reports the Re number of AASSs and gaseous mixture. As the results demonstrate, the Re numbers in both tube and shell pathways of HMC are much lower than 2100, which verifies the assumption of laminar flow regime in the tube and the shell sides of HMC.

5. Results and discussion

5.1. Model validation

To validate the obtained results of modeling and simulation, model's predictions for CO₂ molecular sequestration in a specified range of gas flow are compared with literature data achieved by Yan et al. for PG and MEA solutions (Yan et al., 2007). As shown in Fig. 2, illustrious agreement between the modeling/simulation results and experimental data with average deviation of approximately 3% implies the validation of employed numerical modeling and axisymmetrical simulation. Moreover, it is observed that separation efficiency is reduced with increasing the gas flow velocity in the shell side, which is due to shorter residence time.

5.2. Study of CO₂ concentration gradient and CO₂ molecular sequestration percentage

Fig. 3 aims to illustrate the CO₂ concentration gradient inside the shell pathway of HMC. Due to the counter-current movement of gaseous mixture - AASSs inside the HMC, the feed gas enters the module from the bottom (at $z = 0$, where the CO₂ concentration is adjusted to be maximum) and the flowing of AASSs including PT, PG, PS and PL from the top of the module (at $z = L$, where the CO₂ concentration is proffered to be zero). The sequestration process of CO₂ molecules from the inlet gaseous mixture would be appropriately justified by the CO₂ molecular transfer from shell side to membrane micropores, and their absorption by AASSs in the tube pathway. Comparison of the CO₂ concentration content in the inlet

Table 3 Reynolds numbers in the tube and shell pathways of HMC.

Reynolds number	Re _{PG}	Re _{PL}	Re _{PT}	Re _{PS}	Re _{gaseousmixture}
Tubewise	19.06	12.83	16.01	62.3	–
Shellside				–	7.27

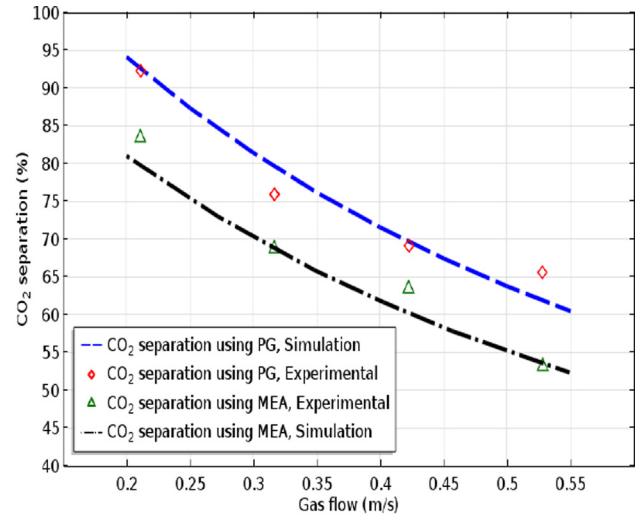


Fig. 2 Comparison between model predictions and experimental data for CO₂ separation in a wide range of gas flow applying PG and MEA solution. Experimental data was made by Yan et al. (2007).

and outlet of shell pathway implies the superiority of PG for CO₂ molecular sequestration with the ability of separating about 90% of inlet CO₂. Based on the comparison, the sequestration percentage of CO₂ using PT, PL and PS amino acid salt solutions is 89.3, 77.4 and 72.3%, respectively. Therefore, PG solution is introduced as the most efficacious amino acid solution for sequestering CO₂ from gaseous mixtures.

5.3. Study of AASSs concentration gradient at the tube-membrane interface

Concentration gradient of AASSs including PT, PG, PS and PL alongside the HMC's tube-membrane interface on the basis of non-wetted operational mode is demonstrated in Fig. 4. Whene CO₂ molecules diffuse inside the membrane micropores, they react with PT, PG, PS and PL amino acid solutions, which are simultaneously circulating in the tube pathway. At the tube-membrane interface, concentration content of PT, PS, PG and PL solutions declines significantly due to the CO₂ molecules - AASSs reaction and also their consumption. It can be shown from the figure that approximately all of PT, PS, PG and PL solutions are consumed and their contents are zero at the tube-membrane interface, which implies the fast reaction of CO₂ molecules with AASSs.

5.4. Study of design/oprational parameters effects on the CO₂ molecular sequestration

The percentage of CO₂ molecular sequestration is derived by the following equation (Cussler, 2009; Nakhjiri and Heydarinasab, 2020b; Nakhjiri et al., 2018a):

$$\begin{aligned} \text{Sequestration}\% &= 100 \left(\frac{(vC)_{inlet} - (vC)_{outlet}}{(vC)_{inlet}} \right) \\ &= 100 \left(\frac{(Q\varphi)_{inlet} - (Q\varphi)_{outlet}}{(Q\varphi)_{inlet}} \right) \\ &= 100 \left(1 - \frac{C_{outlet}}{C_{inlet}} \right) \end{aligned} \quad (29)$$

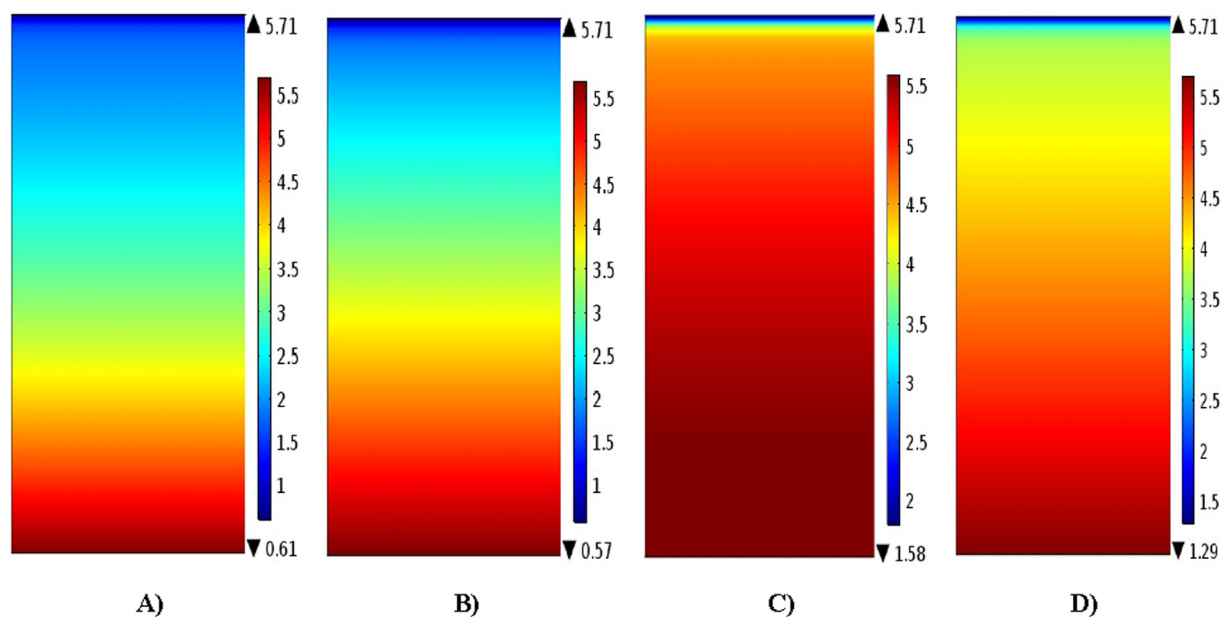


Fig. 3 CO_2 concentration gradient in the shell pathway of HMC using A) PT, B) PG, C) PS and D) PL solutions. CO_2 volume fraction in feed gas = 14 vol% (equal with 5.71 mol m^{-3}), $V_1 = 0.0503 \text{ m s}^{-1}$, $V_g = 0.211 \text{ m s}^{-1}$, $C_{\text{AASSs}} = 1000 \text{ mol m}^{-3}$, $T = 308 \text{ K}$.

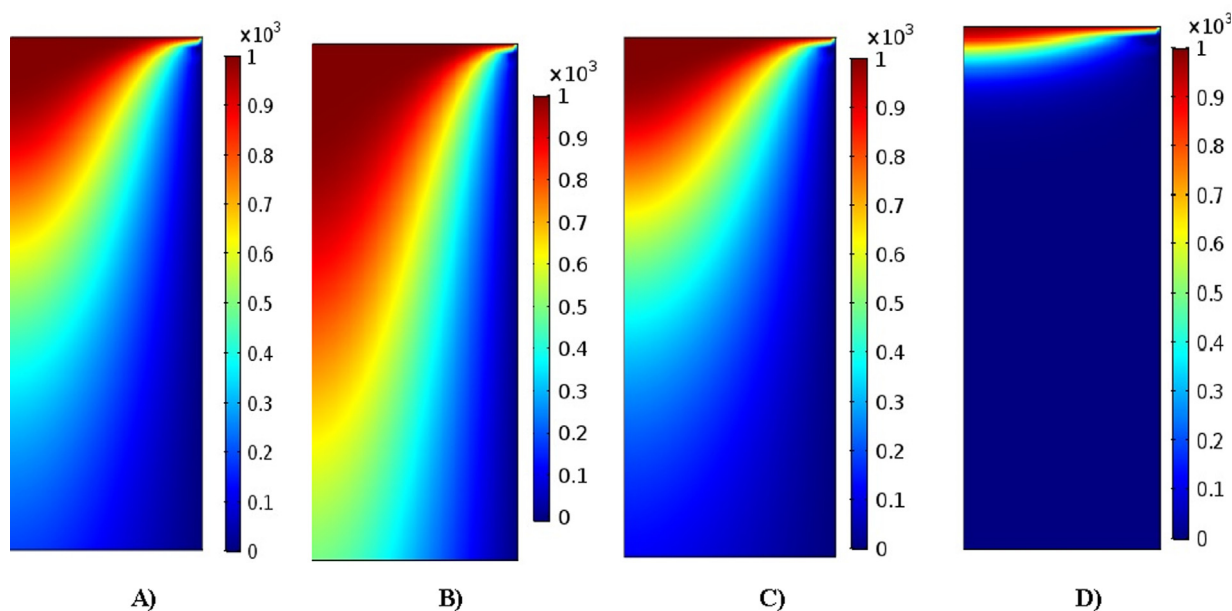


Fig. 4 Concentration gradient of A) PT, B) PG, C) PS and D) PL solutions at the tube-membrane interface. CO_2 volume fraction in feed gas = 14 vol% (equal with 5.71 mol m^{-3}), $V_1 = 0.0503 \text{ m s}^{-1}$, $V_g = 0.211 \text{ m s}^{-1}$, $C_{\text{AASSs}} = 1000 \text{ mol m}^{-3}$, $T = 308 \text{ K}$.

The module length's influence on the molecular sequestration efficiency of CO_2 applying AASSs including PT, PG, PS and PL based on the non-wetted operational mode is depicted in Fig. 5. As would be expected, the sequestration efficiency of CO_2 molecules from gaseous mixture increases dramatically by increasing the module length. This increment can be associated with increasing the contact area inside the module and also enhancement of residence time for both phases. It is shown from the figure that increase in the module length from 0.2 to 1.4 m enhances the sequestration efficiency of CO_2 molecules from 50 to 95% using PG, from 43 to 95% using PT, from 33 to 85% using PL and from 32 to 78% using PS.

The influence of membrane porosity on the sequestration percentage of CO_2 molecules utilizing AASSs including PT, PG, PS and PL is demonstrated in Fig. 6. As mentioned in Eq. (14), a direct connection exists between the porosity content of membrane and the effective diffusivity of CO_2 molecules in the membrane pathway ($D_{\text{CO}_2\text{-mem}}$) (Faiz and Al-Marzouqi, 2009; Gabelman and Hwang, 1999). This equation demonstrates that increase in the porosity of membrane eventuates in a significant improvement in the effective diffusivity of CO_2 molecules in the membrane pathway. As a result, by enhancing the effective diffusivity of CO_2 molecules, the molecular mass transfer of CO_2 inside the membrane pathway

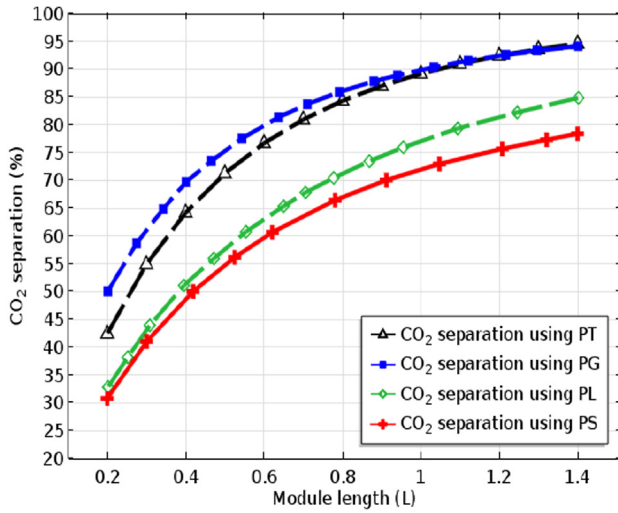


Fig. 5 The module length's effect on the CO₂ molecular sequestration percentage using PT, PG, PS and PL solutions. CO₂ volume fraction in feed gas = 14 vol% (equal with 5.71 mol m⁻³), V₁ = 0.0503 m s⁻¹, V_g = 0.211 m s⁻¹, C_{AASSs} = 1000 mol m⁻³, T = 308 K.

remarkably improves which causes the increase in the sequestration yield of CO₂ molecules in the HMC. The aforementioned figure shows that enhancement of the porosity of membrane from 0.1 to 0.9 improves the sequestration efficiency of CO₂ molecules from 70 to 98.5% using PG, from 67.5 to 98% using PT, from 38 to 95% using PL and from 26 to 94% using PS.

The sequestration efficiency of CO₂ molecules using different AASSs in an extensive range of tortuosity (from 2 to 6) can be presented by Fig. 7. It is worth mentioning that the membrane's tortuosity in this paper is calculated 5.339 using the following equation (Nabipour et al., 2020; Pishnamazi et al., 2020c, 2020e; Srisurichan et al., 2006):

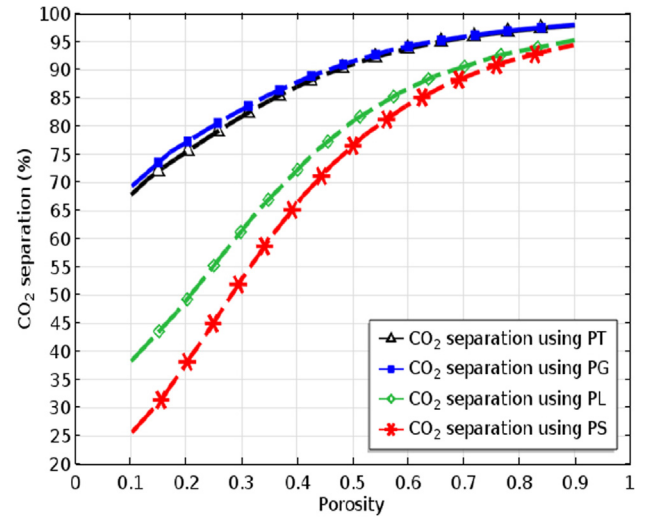


Fig. 6 The effect of membrane porosity on the CO₂ molecular sequestration percentage using PT, PG, PS and PL solutions. CO₂ volume fraction in feed gas = 14 vol% (equal with 5.71 mol m⁻³), V₁ = 0.0503 m s⁻¹, V_g = 0.211 m s⁻¹, C_{AASSs} = 1000 mol m⁻³, T = 308 K.

$$\tau = (2 - \varepsilon)^2 / \varepsilon \quad (30)$$

It is well perceived that increment of membrane tortuosity intensifies the membrane mass transfer resistance, which causes a remarkable deterioration in the CO₂ molecular mass transfer. Consequently, the reduction of CO₂ molecular mass transfer inside the micropores of membrane negatively affects the CO₂ sequestration percentage.

6. Conclusions

The prominent purpose of this study is to compare the performance of four promising amino acid salt solutions including

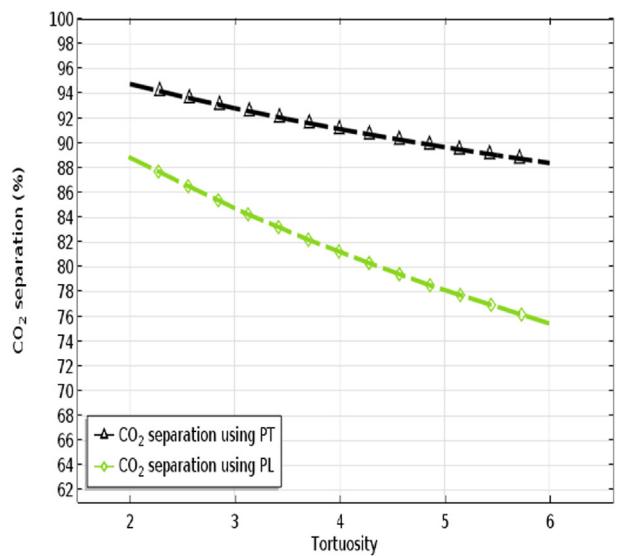
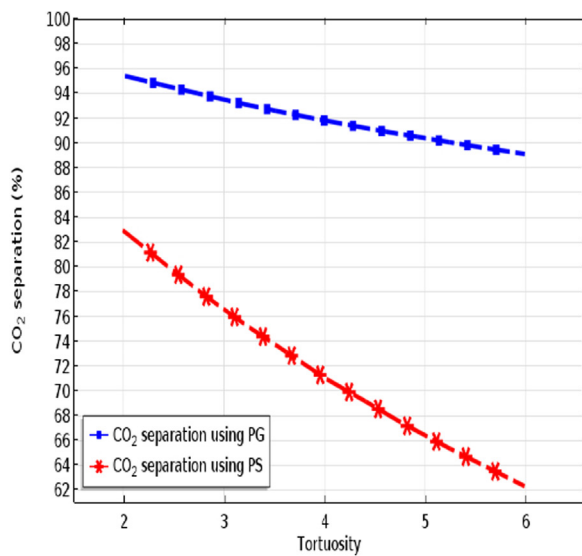


Fig. 7 The effect of membrane tortuosity on the CO₂ molecular sequestration percentage using PT, PG, PS and PL solutions. CO₂ volume fraction in feed gas = 14 vol% (equal with 5.71 mol m⁻³), V₁ = 0.0503 m s⁻¹, V_g = 0.211 m s⁻¹, C_{AASSs} = 1000 mol m⁻³, T = 308 K.

PG, PL, PS and PT for sequestering CO₂ molecules from an inlet gaseous stream inside a HMC. To do this, a numerical modeling and a computational 2D axisymmetrical simulation are developed based on the computational fluid dynamics (CFD) procedure to analyze and solve the governing mass/momentum transfer equations inside the main compartments of HMC. After analyzing the results, it is well identified that PG is the most efficient amino acid solution for CO₂ molecular sequestration with the ability of sequestering 90% of inlet CO₂ to the system. The order of solutions is 90% sequestration using PG > 89.3% sequestration using PT > 77.4% sequestration using PL > 72.3% sequestration using PS at the optimum condition. Therefore, it can be claimed that PG and even PT may be considered as promising alternatives for conventional alkanolamine solutions to mitigate the anthropogenic emission of CO₂ molecules into the natural environment. Moreover, the results showed the positive influence of increasing some operational parameters such as length of module and porosity on the sequestration efficiency of CO₂ molecules, and also the negative impact of increasing the amount of tortuosity on the CO₂ sequestration percentage.

Declaration of Competing Interest

The authors declare that they have no known competing financial interests or personal relationships that could have appeared to influence the work reported in this paper.

Acknowledgement

S.S. acknowledges the supports by the Government of the Russian Federation (Act 211, contract 02.A03.21.0011) and by the Ministry of Science and Higher Education of Russia (grant FENU-2020-0019).

References

- Afza, K.N., Hashemifard, S., Abbasi, M., 2018. Modelling of CO₂ absorption via hollow fiber membrane contactors: Comparison of pore gas diffusivity models. *ChEnS* 190, 110–121.
- Al-Marzouqi, M., El-Naas, M., Marzouk, S., Abdullatif, N., 2008a. Modeling of chemical absorption of CO₂ in membrane contactors. *Sep. Purif. Technol.* 62, 499–506.
- Al-Marzouqi, M.H., El-Naas, M.H., Marzouk, S.A., Al-Zarooni, M. A., Abdullatif, N., Faiz, R., 2008b. Modeling of CO₂ absorption in membrane contactors. *Sep. Purif. Technol.* 59, 286–293.
- Aronu, U.E., Hartono, A., Hoff, K.A., Svendsen, H.F., 2011. Kinetics of carbon dioxide absorption into aqueous amino acid salt: potassium salt of sarcosine solution. *Ind. Eng. Chem. Res.* 50, 10465–10475.
- Bar-Meir, G., 2014. Basics of Fluid Mechanics. Potto Project, USA.
- Bird, R.B., Stewart, W.E., Lightfoot, E.N., 1960. Transport phenomena. Madison, USA.
- Blauwhoff, P., Versteeg, G., Van Swaaij, W.P.M., 1983. A study on the reaction between CO₂ and alkanolamines in aqueous solutions. *ChEnS* 38, 1411–1429.
- Caplow, M., 1968. Kinetics of carbamate formation and breakdown. *J. Am. Chem. Soc.* 90, 6795–6803.
- Constantinou, A., Barrass, S., Gavriilidis, A., 2014. CO₂ absorption in polytetrafluoroethylene membrane microstructured contactor using aqueous solutions of amines. *Ind. Eng. Chem. Res.* 53, 9236–9242.
- Crooks, J.E., Donnellan, J.P., 1989. Kinetics and mechanism of the reaction between carbon dioxide and amines in aqueous solution. *J. Chem. Soc., Perkin Trans. 2*, 331–333.
- Cussler, E.L., 2009. Diffusion: mass transfer in fluid systems. Cambridge University Press.
- Danckwerts, P.V., 1979. The Reaction of CO₂ with Ethanolamines. *ChEnS* 34, 443–446.
- Demontigny, D., Tontiwachwuthikul, P., Chakma, A., 2005. Comparing the absorption performance of packed columns and membrane contactors. *Ind. Eng. Chem. Res.* 44, 5726–5732.
- Eslami, S., Mousavi, S.M., Danesh, S., Banazadeh, H., 2011. Modeling and simulation of CO₂ removal from power plant flue gas by PG solution in a hollow fiber membrane contactor. *Adv. Eng. Software* 42, 612–620.
- Faiz, R., Al-Marzouqi, M., 2009. Mathematical modeling for the simultaneous absorption of CO₂ and H₂S using MEA in hollow fiber membrane contactors. *J. Membr. Sci.* 342, 269–278.
- Feron, P., Jansen, A., Klaassen, R., 1992. Membrane technology in carbon dioxide removal. *Energy Convers. Manage.* 33, 421–428.
- Gabelman, A., Hwang, S.-T., 1999. Hollow fiber membrane contactors. *J. Membr. Sci.* 159, 61–106.
- Ghadiri, M., Mohammadi, M., Asadollahzadeh, M., Shirazian, S., 2018. Molecular separation in liquid phase: Development of mechanistic model in membrane separation of organic compounds. *J. Mol. Liq.* 262, 336–344.
- Ghasem, N., Al-Marzouqi, M., 2017. Modeling and experimental study of carbon dioxide absorption in a flat sheet membrane contactor. *J. Membr. Sci. Res.* 3, 57–63.
- Hamborg, E.S., van Swaaij, W.P., Versteeg, G.F., 2008. Diffusivities in aqueous solutions of the potassium salt of amino acids. *J. Chem. Eng. Data* 53, 1141–1145.
- Herzog, H., Eliasson, B., Kaarstad, O., 2000. Capturing greenhouse gases. *SciAm* 282, 72–79.
- Kim, Y.-S., Yang, S.-M., 2000. Absorption of carbon dioxide through hollow fiber membranes using various aqueous absorbents. *Sep. Purif. Technol.* 21, 101–109.
- Kreulen, H., Smolders, C., Versteeg, G., Van Swaaij, W.P.M., 1993. Determination of mass transfer rates in wetted and non-wetted microporous membranes. *ChEnS* 48, 2093–2102.
- Kumar, P., Hogendoorn, J., Versteeg, G., Feron, P., 2003. Kinetics of the reaction of CO₂ with aqueous potassium salt of taurine and glycine. *AIChE* 49, 203–213.
- Li, S., Shou, S., Pyrzyński, T., Makkuni, A., Meyer, H., 2013. Hybrid Membrane/Absorption Process for Post-combustion CO₂ Capture, Institute Of Gas Technology.
- Lu, J.-G., Fan, F., Liu, C., Zhang, H., Ji, Y., Chen, M.-d., 2011. Density, viscosity, and surface tension of aqueous solutions of potassium glycinate + piperazine in the range of (288.15 to 323.15) K. *J. Chem. Eng. Data* 56, 2706–2709.
- Majchrowicz, M.E., 2014. Amino acid Salt Solutions for Carbon Dioxide Capture. University of Twente.
- Mazinani, S., Ramazani, R., Samsami, A., Jahanmiri, A., Van der Bruggen, B., Darvishmanesh, S., 2015. Equilibrium solubility, density, viscosity and corrosion rate of carbon dioxide in potassium lysinate solution. *Fluid Phase Equilib.* 396, 28–34.
- Mehdipour, M., Keshavarz, P., Seraji, A., Masoumi, S., 2014. Performance analysis of ammonia solution for CO₂ capture using microporous membrane contactors. *Int. J. Greenhouse Gas Control* 31, 16–24.
- Nabipour, N., Babanezhad, M., Taghvaei Nakhjiri, A., Shirazian, S., 2020. Prediction of nanofluid temperature inside the cavity by integration of grid partition clustering categorization of a learning structure with the fuzzy system. *ACS omega* 5, 3571–3578.
- Naim, R., Ismail, A., Mansourizadeh, A., 2012. Preparation of microporous PVDF hollow fiber membrane contactors for CO₂ stripping from diethanolamine solution. *J. Membr. Sci.* 392, 29–37.

- Nakhjiri, A.T., Roudsari, M.H., 2016. Modeling and simulation of natural convection heat transfer process in porous and non-porous media. *Appl. Res. J.* 2, 199–204.
- Nakhjiri, A.T., Heydarinasab, A., Bakhtiari, O., Mohammadi, T., 2018a. Modeling and simulation of CO₂ separation from CO₂/CH₄ gaseous mixture using potassium glycinate, potassium arginate and sodium hydroxide liquid absorbents in the hollow fiber membrane contactor. *J. Environ. Chem. Eng.* 6, 1500–1511.
- Nakhjiri, A.T., Heydarinasab, A., Bakhtiari, O., Mohammadi, T., 2018b. Experimental investigation and mathematical modeling of CO₂ sequestration from CO₂/CH₄ gaseous mixture using MEA and TEA aqueous absorbents through polypropylene hollow fiber membrane contactor. *J. Membr. Sci.* 565, 1–13.
- Nakhjiri, A.T., Heydarinasab, A., Bakhtiari, O., Mohammadi, T., 2018c. The effect of membrane pores wettability on CO₂ removal from CO₂/CH₄ gaseous mixture using NaOH, MEA and TEA liquid absorbents in hollow fiber membrane contactor. *Chin. J. Chem. Eng.* 26, 1845–1861.
- Nakhjiri, A.T., Heydarinasab, A., 2019. Computational simulation and theoretical modeling of CO₂ separation using EDA, PZEA and PS absorbents inside the hollow fiber membrane contactor. *J. Indust. Eng. Chem.* 78, 106–115.
- Nakhjiri, A.T., Heydarinasab, A., 2020a. CFD analysis of CO₂ sequestration applying different absorbents inside the microporous PVDF hollow fiber membrane contactor. *Periodica Polytech. Chem. Eng.* 64, 135–145.
- Nakhjiri, A.T., Heydarinasab, A., 2020b. Efficiency evaluation of novel liquid potassium lysinate chemical solution for CO₂ molecular removal inside the hollow fiber membrane contactor: comprehensive modeling and CFD simulation. *J. Mol. Liq.* 297, 111561.
- Nakhjiri, A.T., Heydarinasab, A., Bakhtiari, O., Mohammadi, T., 2020. Numerical simulation of CO₂/H₂S simultaneous removal from natural gas using potassium carbonate aqueous solution in hollow fiber membrane contactor. *J. Environ. Chem. Eng.*, 104130
- Park, H.H., Deshwal, B.R., Jo, H.D., Choi, W.K., Kim, I.W., Lee, H. K., 2009. Absorption of nitrogen dioxide by PVDF hollow fiber membranes in a G-L contactor. *Desalination* 243, 52–64.
- Pishnamazi, M., Nakhjiri, A.T., Ghadiri, M., Marjani, A., Heydarinasab, A., Shirazian, S., 2020a. Computational fluid dynamics simulation of NO₂ molecular sequestration from a gaseous stream using NaOH liquid absorbent through porous membrane contactors. *J. Mol. Liq.*, 113584
- Pishnamazi, M., Nakhjiri, A.T., Marjani, A., Taleghani, A.S., Reza-kazemi, M., Shirazian, S., 2020b. Computational study on SO₂ molecular separation applying novel EMISE ionic liquid and DMA aromatic amine solution inside microporous membranes. *J. Mol. Liq.*, 113531
- Pishnamazi, M., Nakhjiri, A.T., Taleghani, A.S., Marjani, A., Heydarinasab, A., Shirazian, S., 2020c. Computational investigation on the effect of [Bmim][BF₄] ionic liquid addition to MEA alkaline absorbent for enhancing CO₂ mass transfer inside membranes. *J. Mol. Liq.*, 113635
- Pishnamazi, M., Taghvaie Nakhjiri, A., Rezakazemi, M., Marjani, A., Shirazian, S., 2020d. Mechanistic modeling and numerical simulation of axial flow catalytic reactor for naphtha reforming unit. *PLoS One* 15, e0242343.
- Pishnamazi, M., Taghvaie Nakhjiri, A., Sodagar Taleghani, A., Ghadiri, M., Marjani, A., Shirazian, S., 2020e. Molecular separation of ibuprofen and 4-isobutylacetophenone using octanol organic solution by porous polymeric membranes. *PLoS One* 15, e0237271.
- Portugal, A., Derks, P., Versteeg, G., Magalhaes, F., Mendes, A., 2007a. Characterization of potassium glycinate for carbon dioxide absorption purposes. *Chem. Eng. Sci.* 62, 6534–6547.
- Portugal, A., Derks, P., Versteeg, G., Magalhães, F., Mendes, A., 2007b. Characterization of potassium glycinate for carbon dioxide absorption purposes. *ChEnS* 62, 6534–6547.
- Portugal, A., Magalhaes, F., Mendes, A., 2008. Carbon dioxide absorption kinetics in potassium threonate. *ChEnS* 63, 3493–3503.
- Portugal, A., Sousa, J., Magalhães, F., Mendes, A., 2009. Solubility of carbon dioxide in aqueous solutions of amino acid salts. *Chem. Eng. Sci.* 64, 1993–2002.
- Razavi, S.M.R., Razavi, S.M.J., Miri, T., Shirazian, S., 2013. CFD simulation of CO₂ capture from gas mixtures in nanoporous membranes by solution of 2-amino-2-methyl-1-propanol and piperazine. *Int. J. Greenhouse Gas Control* 15, 142–149.
- Razavi, S.M.R., Shirazian, S., Nazemian, M., 2016. Numerical simulation of CO₂ separation from gas mixtures in membrane modules: effect of chemical absorbent. *Arab. J. Chem.* 9, 62–71.
- Rongwong, W., Assabumrungrat, S., Jiraratananon, R., 2013. Rate based modeling for CO₂ absorption using monoethanolamine solution in a hollow fiber membrane contactor. *J. Membr. Sci.* 429, 396–408.
- Rufford, T.E., Smart, S., Watson, G.C., Graham, B., Boxall, J., Da Costa, J.D., May, E., 2012. The removal of CO₂ and N₂ from natural gas: a review of conventional and emerging process technologies. *J. Petrol. Sci. Eng.* 94, 123–154.
- Shen, S., Feng, X., Zhao, R., Ghosh, U.K., Chen, A., 2013. Kinetic study of carbon dioxide absorption with aqueous potassium carbonate promoted by arginine. *Chem. Eng. J.* 222, 478–487.
- Shen, S., Yang, Y-n, Bian, Y., Zhao, Y., 2016. Kinetics of CO₂ absorption into aqueous basic amino acid salt: potassium salt of lysine solution. *Environ. Sci. Technol.* 50, 2054–2063.
- Shirazian, S., Marjani, A., Rezakazemi, M., 2012. Separation of CO₂ by single and mixed aqueous amine solvents in membrane contactors: fluid flow and mass transfer modeling. *Eng. Comput.* 28, 189–198.
- Shirazian, S., Taghvaie Nakhjiri, A., Heydarinasab, A., Ghadiri, M., 2020. Theoretical investigations on the effect of absorbent type on carbon dioxide capture in hollow-fiber membrane contactors. *PLoS One* 15, e0236367.
- Srisurichan, S., Jiraratananon, R., Fane, A., 2006. Mass transfer mechanisms and transport resistances in direct contact membrane distillation process. *J. Membr. Sci.* 277, 186–194.
- van Holst, J., Versteeg, G., Brilman, D.W.F., Hogendoorn, J., 2009. Kinetic study of CO₂ with various amino acid salts in aqueous solution. *ChEnS* 64, 59–68.
- Yan, S-p, Fang, M.-X., Zhang, W.-F., Wang, S.-Y., Xu, Z.-K., Luo, Z.-Y., Cen, K.-F., 2007. Experimental study on the separation of CO₂ from flue gas using hollow fiber membrane contactors without wetting. *Fuel Process. Technol.* 88, 501–511.
- Zhang, Z., Yan, Y., Zhang, L., Chen, Y., Ju, S., 2014. CFD investigation of CO₂ capture by methyldiethanolamine and 2-(1-piperazinyl)-ethylamine in membranes: Part B. Effect of membrane properties. *J. Natural Gas Sci. Eng.* 19, 311–316.
- Zhang, Z., 2016. Comparisons of various absorbent effects on carbon dioxide capture in membrane gas absorption (MGA) process. *J. Nat. Gas Sci. Eng.* 31, 589–595.
- Zhou, S.J., Li, S., Meyer, H., Ding, Y., Bikson, B., 2010. Hybrid membrane absorption process for post combustion CO₂ capture. In: 2010 Spring Meeting & 6th Global Congress on Process Safety, AIChE, San Antonio, Texas.